ChemComm

COMMUNICATION

View Article Online
View Journal | View Issue

Cite this: *Chem. Commun.*, 2019, 55, 8880

Received 7th June 2019,
Accepted 3rd July 2019

DOI: 10.1039/c9cc04388h

rsc.li/chemcomm

Artificial β-propeller protein-based hydrolases†

David E. Clarke, ‡[ab] Hiroki Noguchi, ‡[b] Jean-Louis A. G. Gryspeerdt,[b] Steven De Feyter [a] and Arnout R. D. Voet *[b]

We developed an artificial hydrolase based on the symmetrical Pizza6 β-propeller protein for the metal-free hydrolysis of 4-nitrophenyl acetate and butyrate. Through site-specific mutagenesis and crystallisation studies, the catalytic mechanism was investigated and found to be dependent on a threonine–histidine dyad. The mutant with additional histidine residues generated the highest k_{cat} values, forming a His–His–Thr triad and matched previously reported metalloenzymes. The highly symmetrical β-propeller artificial enzymes and their protein–metal complexes have potential to be utilised in bioinorganic and supramolecular chemistry, as well as being developed further into 2D/3D catalytic materials.

The ability to design and tune artificial enzymes to perform desired chemical reactions has considerable practical applications in biocatalysis.[1,2] Advancements in protein design have provided a platform for the generation of proteins with unique folds and interfaces.[1,3] This has enabled designer artificial proteins to perform unique functions, including the catalytic rate enhancement of specific chemical reactions. Artificial protein-based enzymes are often asymmetric in structure which allow them to catalyse a number of challenging chemical reactions, including those not found in nature.[1,4–6] Moreover, a range of approaches have been developed to optimise them for chemo-, regio-, site-, and enantioselective catalysis.[2,5]

The typical structures of these artificial proteins are derived from α-helical bundles/β-sheet domains or oligomeric extended peptide structures that are coupled with metallo-cofactors.[7–13] These catalytically active metal ions have been incorporated through the design of both natural histidine-mediated[7,8,12] and artificial binding sites.[14–16] Specifically, peptide/protein-zinc complexes have been demonstrated as powerful catalysts in hydrolysis reactions, where the presence of a zinc ion was found to provide an activated water molecule for nucleophilic attack, as well as stabilising the substrate-catalysis transition state.[8–12] Proteins have also been combined with other metal ions such as copper(II) to perform enantioselective catalysis, mimicking both a hydratase,[15,16] and a Diels–Alderase.[7,14]

Outside of these metalloenzymes, there have been a few attempts to formulate artificial proteins that can perform metal-free hydrolysis.[17,18] This is quite surprising given that the active-sites of natural α/β-hydrolases are metal-free.[19] Furthermore, the majority of artificial enzymes are fabricated from asymmetric protein structures, with only a few examples that have utilised alternative geometries, such as the highly symmetrical β-propeller structure.[5,20] In two examples, β-propeller proteins have successfully been combined with an additional foldable lid to generate a Diels–Alderase,[20] and with a dirhodium catalyst to catalyse olefin cyclopropanation.[5] The development of artificial enzymes formulated from symmetrical protein structures holds great promise in supramolecular catalysis.[12,21] These symmetrical geometries can be utilised as catalytic building blocks to construct higher order 2D/3D materials such as surface arrays and cages.[12]

Previously, we reported the design and synthesis of a symmetrical β-propeller protein named Pizza6.[22] The Pizza6 protein consists of six tandem repeats of 42 amino acids (AAs) and folds into a geometry with six-fold symmetry (Fig. 1). The central axis of Pizza6 has also been modified to coordinate the formation of a cadmium chloride nanocrystal sandwiched between two Pizza β-propeller units.[23] To develop Pizza6 towards catalytic applications, the Pizza6-SH and Pizza6-S mutants were designed to generate different histidine (His) configurations (Fig. 1 and Fig. S2, ESI†). Through the crystallography of these mutants, we studied their binding with two metal ions widely used in biocatalysis (copper and zinc), which have a strong affinity for His residues (detailed crystallographic data can be found in the Fig. S1 and S3, ESI†).

[a] *Division of Molecular Imaging and Photonics, Department of Chemistry, KU Leuven, Celestijnenlaan 200F, 3001, Leuven, Belgium*
[b] *Laboratory of Biomolecular Modelling and Design, Department of Chemistry, KU Leuven, Celestijnenlaan 200G, 3001 Leuven, Belgium. E-mail: arnout.voet@kuleuven.be*

† Electronic supplementary information (ESI) available. See DOI: 10.1039/c9cc04388h

‡ These authors contributed equally to this work.

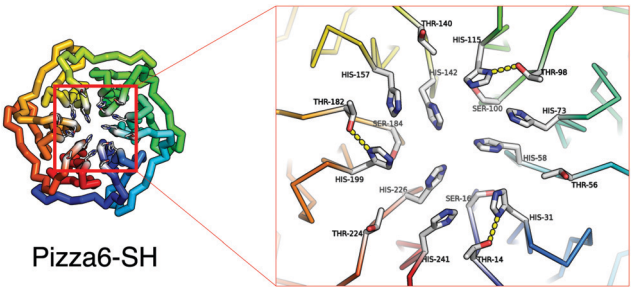

Fig. 1 Structure of the artificial Pizza6-SH hydrolase with the amino acids surrounding the cavity magnified (right).

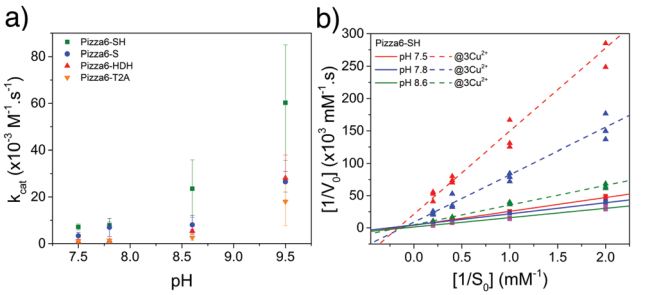

Fig. 2 (a) pH dependency of k_{cat} for the hydrolysis of *p*-NPA by the different Pizza6 proteins. (b) Lineweaver–Burk (double-reciprocal) plots of the Pizza6-SH and Pizza6-SH@3Cu^{2+} complex (pH 7.5–8.6), demonstrating that the Cu^{2+} ions act as non-competitive inhibitors.

The Pizza6-S mutant contains 6 His residues surrounding its cavity and was created from the original Pizza6 protein by mutating the asparagine at positions 16, 100 and 184 to serine (Ser) (Fig. S2, ESI†). This mutant was found to dimerize in the presence of copper and zinc forming a metal-ion ring-like structure between two proteins (Fig. S1, S3 and S5, ESI†). Interestingly, the Pizza6-SH mutant with 9 His residues on its top-side (Fig. 1) generated three viable metal binding sites that existed in a monomeric configuration. These binding sites in Pizza6-SH mutant demonstrated the complexation of both Cu^{2+} and Zn^{2+}, where each metal ion was coordinated by 3 His residues and was surrounded by a high density of water molecules or isopropanol (Fig. S1, S3 and S4, ESI†). The native geometry of Pizza6 also provides $\approx$0.56 nm^3 cavity, which combined with a metal-binding site serves as an ideal platform to investigate as an artificial enzyme. With this in mind, we investigated the utilisation of Pizza6 mutants and their metal complexes as an artificial hydrolase, studying the hydrolysis of the small model compounds 4-nitrophenyl acetate/butyrate/phosphate (*p*-NPA/*p*-NPB/*p*-NPP) as a model reaction.

In an initial study, we trialed the Pizza6-SH protein along with metal complexes of 3 eq. of zinc (Pizza6SH@3Zn^{2+}) or copper (Pizza6SH@3Cu^{2+}) as artificial hydrolases. To evaluate these catalysts, we studied the reaction kinetics at pH 7.0–9.5 and found that typical saturation kinetics were exhibited for *p*-NPA hydrolysis in buffered aqueous solution (Fig. S14, ESI†). Surprisingly, the Pizza6-SH protein was found to generate a significant rate enhancement in the hydrolysis of *p*-NPA when compared to the Pizza6-SH@3Zn^{2+}/Pizza6-SH@3Cu^{2+} complexes especially at pH 7.0–8.6 (Table S4 and Fig. S8–S10, ESI†), with the protein alone obtaining k_{cat} = 7.83($\pm$1.45) $\times$ 10^{-3} s^{-1} and k_{cat}/K_M = 1.50($\pm$0.05) M^{-1} s^{-1} at pH 7.5 (25 °C, 30 μM catalyst, Table S4, ESI†). We also observed an increase in both the rate and catalytic efficiencies of the Pizza6-SH with increasing pH, where k_{cat} increased 7 fold and a k_{cat}/K_M = 4.74($\pm$0.12) M^{-1} s^{-1} was reached at pH 9.5 (Fig. 2a and Fig. S15, Table S4, ESI†). This observation was surprising given the previous success of peptide/protein-zinc complexes.[8–12] However, it inspired us to investigate the mechanism of the Pizza6-SH protein and its inherent capability as a metal-free hydrolase. We hypothesised that by utilising the modularity of the protein and through specific mutations, we could study the mechanistic influence of the residues surrounding the cavity in an attempt to improve the hydrolytic efficiency of the protein (Fig. 1).

The residues typically used in natural enzymes for nucleophile-catalysed hydrolysis are based around a triad composed of Ser, His and aspartic acid (Asp), which act as nucleophile, base and an acid respectively. This Ser–His–Asp catalytic triad combined with an oxyanion hole is known to catalyse a large diversity of reactions with widely varying mechanisms.[19] In addition, previous reports have demonstrated the importance of His which can act as either an acid or base, and also as a nucleophile, forming acylated-intermediates which promote turnover and product formation.[17,24,25] The structure of the Pizza6-SH protein contains a 9 His ring which is surrounded by neighbouring threonine (Thr) residues (Fig. 1). This combination of AAs potentially generates catalytic Thr–His dyads, as Thr is similar in structure to Ser. Alternatively, given the flexibility of His to perform either as a base or an acid, a Thr–His–His triad could be formed with a neighbouring His acting as an acid.

To evaluate the role of the His residues in both the catalytic mechanism and efficiency, we investigated two additional mutants as hydrolases: Pizza6-S and 1RWL,[22] the naturally occurring pseudo-symmetric parent structure of the Pizza proteins (Fig. S2, ESI†). 1RWL has both a single His and Thr on its top axis, but was found to have no catalytic activity. The Pizza6-S mutant contains 6 His residues surrounding its cavity along with the same neighbouring Thr(s), whilst maintaining a native 6-fold symmetry (Fig. S2, ESI†). Similarly, the Pizza6-S mutant generated a significant rate enhancement in the hydrolysis of the *p*-NPA esters and displayed typical saturation kinetics (Table S4, ESI†). The same increase in both the rate and catalytic efficiencies as pH is increased from pH 7.0 to pH 9.5 was also observed (Fig. 2a and Fig. S15, Table S4, ESI†). Comparing the kinetic parameters of the Pizza6-S and Pizza6-SH proteins, we found that the additional His residues in the Pizza6-SH protein improved the performance of the catalyst in relation to k_{cat}. We also observed a difference in K_M; for Pizza6-S the K_M remains roughly constant and within error as the pH increases (Table S4, ESI†). Conversely, for the Pizza6-SH protein, K_M increases as pH $>$ 7.8 and thus, results in only a modest increase in k_{cat}/K_M at the higher pH range (Table S4, ESI†). This suggests that the additional His plays an important mechanistic role in the Pizza6-SH protein, but it can

also generate a weaker affinity with the starting material when deprotonated at higher pH.

In an attempt to further optimise the hydrolase, we investigated the introduction of Asps into the vicinity of the Thr–His dyads to mimic an active Ser–His–Asp triad, which is widely found in natural enzymes.[19] Asps were introduced in to the scaffold in positions 31, 115, 199 (Pizza6-DHH), at 73, 157, 241 (Pizza6-HDH) or at 58, 142, 226 (Pizza6-HHD) to act as an acid to activate the His residues in neighbouring positions (Fig. S2, ESI†). Through moving the Asp to position 31 or 73 and their symmetrical equivalents, in the Pizza6-DHH and Pizza-HDH proteins, we aimed to further ratify our hypothesis that Thr–His dyad are essential to the hydrolase mechanism. These mutations were found to diminish the catalytic activity of Pizza-HDH when compared to the Pizza6-SH scaffold across the entire pH range with the maximum k_{cat} = 28.13(±9.86) × 10^{-3} s^{-1} and k_{cat}/K_M = 2.16(±0.12) M^{-1} s^{-1} achieved at pH 9.5 (25 °C, 30 μM catalyst, Table S4, ESI†). The Pizza6-HDH also displayed the similar behaviour to the Pizza6-SH protein with an increase in K_M observed as pH > 7.8 (Table S4, ESI†). Structurally, the pK_a of Asp is likely to be mediated by interactions with the nearby His, and it appears to deprotonate at pH > 7.8. This acid residue could potentially generate a Asp–His dyad with His31 (and symmetric equivalents), resulting in the substantial rise in k_{cat} at pH 9.5. However, as previously observed, negative charge also has an adverse effect on the affinity of *p*-NPA for the protein. Replacing His by Asp residues in the Pizza6-DHH and Pizza6-HHD protein, were found to not generate any catalytic activity in the hydrolysis of the *p*-NPA ester (Pizza6-HHD did not form a stable protein). In light of this, it can be assumed that the mutation in Pizza6-DHH disrupts the coordination of the active Thr–His dyads and therefore, eliminates its catalytic activity altogether (Fig. S2, ESI†).

We also elected to further investigate the role of Thr14 and symmetric equivalents through mutation to the non-polar alanine (Ala), to provide the Pizza6-T2A mutant (Fig. 1 and Fig. S2, ESI†). As discussed, Thr is similar in structure to Ser and therefore, can potentially act as a nucleophile or as a base. Comparing the kinetic data of the Pizza6-SH and Pizza6-T2A mutants in the hydrolysis of *p*-NPA, we observed a reduction in both k_{cat} and k_{cat}/K_M for the Pizza6-T2A mutant (Table S4, ESI†). Similarly to the other mutants that contain a His at position 58 and equivalent, Pizza6-T2A also displays a rise in K_M as the pH is increased. Therefore, from these observations it can be confirmed that Thr plays an important mechanistic role in the Pizza6-SH hydrolase. However, unlike the role of Ser in natural enzymes, it is likely to be positioning and constraining the imidazole of His31 through hydrogen bonding with the hydroxyl group of Thr14 and their symmetric equivalents (Fig. 1 and Fig. S5, ESI†). This type of stabilisation of active His through negative charges has proven important in other metal-free artificial enzymes.[4] Therefore, we can infer the mechanism proposed in Fig. 3, where the catalytically active Thr–His dyads are only present in 3 of the 6 blades. This is further supported by the Pizza6-DHH mutant, which does not contain these dyads and consequently, has no catalytic activity.

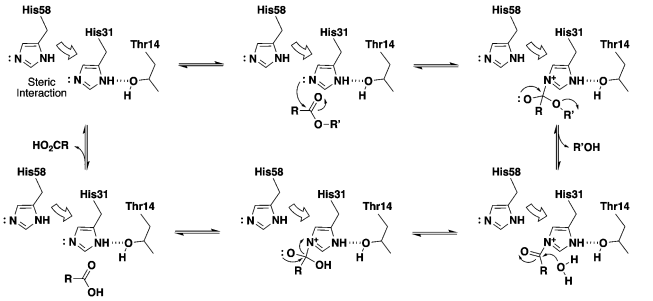

Fig. 3 Proposed mechanism of the Pizza6-SH hydrolase, with His31 acting as the nucleophile constrained by Thr14 and steric interactions from His58.

The chemo-selectivity of the different Pizza6 mutants was studied through the hydrolysis of the alternative *p*-NPB and *p*-NPP esters. Rate enhancement in the hydrolysis of *p*-NPB was observed for the Pizza6-SH, Pizza6-S and Pizza6-T2A scaffolds, but no enhancement was witnessed for the Pizza6-HDH, Pizza6-DHH or Pizza6-HHD mutants (Table S5, ESI†). The reaction kinetics for the hydrolysis of *p*-NPB demonstrated similar behaviour to *p*-NPA with both the rate and catalytic efficiencies increasing with pH (Table S5 and Fig. S16–S19, ESI†). However, the k_{cat} values for all the catalytic proteins dropped by an order of magnitude when compared to the *p*-NPA ester for the same reaction conditions (Fig. S19 and Table S5, ESI†). This was coupled with a significant drop in K_M for the Pizza6-SH and Pizza6-S proteins, leading to similar k_{cat}/K_M for the Pizza6-SH protein for both *p*-NPA (k_{cat}/K_M = 4.74(±0.12) M^{-1} s^{-1}) and *p*-NPB (k_{cat}/K_M = 4.45(±0.45) M^{-1} s^{-1}). This significant reduction in K_M and k_{cat}, suggests that both the Pizza6-SH and Pizza6-S proteins have a greater affinity for the *p*-NPB ester but are less effective in hydrolysing this ester. The Pizza6-T2A mutant behaved differently with respect to K_M, where it maintained a much larger value of K_M = 4.0 mM across the entire pH range. This resulted in the Pizza6-T2A having a lower catalytic efficiency when compared to the other mutants (k_{cat}/K_M = 0.83(±0.07) M^{-1} s^{-1}, pH 9.5). In the case of *p*-NPB, the presence of Thr14 and equivalent appears to influence the substrate affinity as the k_{cat} values for the Pizza6-T2A are in the similar range to both Pizza6-SH and Pizza6-S. For the *p*-NPP ester no catalytic rate enhancement was observed for any of the proteins used in this study.

The kinetic parameters obtained for the protein based hydrolases in this study compare well to the previously reported catalysts for this model reaction, where the k_{cat} values obtained for *p*-NPA are similar in magnitude to artificial zinc-based metalloenzymes (k_{cat} ≈ 12–200 × 10^{-3} s^{-1}).[9–12] Similarly, improved catalytic performance with increasing pH was observed, which highlights the robustness of Pizza6's highly stable β-propeller geometry (Fig. 2a and Fig. S19, ESI†). However, it is apparent that not having a metal ion present results in a weaker affinity for the substrate especially at higher pH. In this case, the zinc ions are likely to provide additional stability in the transition state, especially in basic conditions as negative charges accumulate.[8] The weaker affinity of the Pizza6 mutants

for the substrate caused an increased K_M and consequently, only modest k_{cat}/K_M values are obtained (Table S4, ESI†). In addition, the Pizza6-SH can achieve only a modest fraction of the rate acceleration observed in natural hydrolases, for example the human carbonic anhydrase achieves $k_{cat} \approx 56\ s^{-1}$ under similar reaction conditions.[26]

In the crystal structure of the Pizza6-SH@3Cu^{2+} complex, second-sphere coordinations are observed between the hydroxyl groups of Thr and the metal ions in the His binding site (Fig. S1 and S3, ESI†). The metal ions were found to act as non-competitive inhibitors, where they are unable to provide an activated water molecule and disrupt the Thr–His dyad required for hydrolysis. This was confirmed *via* the double reciprocal plots of the Pizza6-SH and Pizza6-SH@3Cu^{2+} activity, which exhibited typical non-competitive inhibition profiles at pH 7.5–8.6 (Fig. 2b). These inhibitor studies further verified the importance of the Thr–His dyads identified in the crystal structures of the Pizza6-SH and Pizza6-S proteins, and their roles to coordinate and position the nucleophilic His (Fig. 3 and Fig. S6, ESI†). In addition, the site-specific mutagenesis and reaction kinetics suggested that at pH $>$ 7.8 the additional His residues in the Pizza6-SH protein in positions 58, 142 and 226 stabilise the His nucleophiles through steric interactions (Fig. S6, ESI†). This results in the His31 nucleophiles being further constrained and positioned towards Thr14 (Fig. 3).

We report a series of artificial Pizza6 β-propeller proteins that can perform the metal free hydrolysis of the *p*-NPA/*p*-NPB esters. For all the catalytic mutants both the k_{cat} and k_{cat}/K_M were found to increase with pH. To explore the catalytic mechanism we utilised site-specific mutagenesis of the AAs on the top axis, which verified the importance of a Thr–His dyad. The crystal structures and the reaction kinetics of the different Pizza6 mutants suggested that the Thr residues act to position and mediate the His nucleophiles in the dyad through their hydroxyl groups. Unlike previous examples of metalloenzymes, the metal ions in the protein–metal complexes acted as non-competitive inhibitors and disrupted the Thr–His catalytic dyad. The Pizza6-SH mutant was found to generate the highest k_{cat} values of all the mutants, matching previously reported metalloenzymes. Specifically, this mutant contains an additional His which when deprotonated, further positions the His nucleophile and forms a His–His–Thr triad. These symmetrical β-propeller protein enzymes and their metal complexes hold great promise in biocatalysis, where their modular symmetric structure can be explored for more challenging reactions and developed into 2D/3D catalytic materials. In addition, the highly symmetric protein–metal complexes also hold promise in other applications including biomineralisation, bioinorganic and supramolecular chemistry.

The authors acknowledge FWO and KU Leuven (Internal Funds) for funding, and Xiao Yin Lee for assistance in solving the crystal structures. Furthermore, the authors would like to thank Diamond Light Source I04 (proposal mx18582), SOLEIL Proxima-1, Swiss Light Source PXIII and Elettra XRD-1 for beam time and staff for assistance.

Conflicts of interest

There are no conflicts to declare.

Notes and references

1 H. Kries, R. Blomberg and D. Hilvert, *Curr. Opin. Chem. Biol.*, 2013, **17**, 221–228.
2 F. Schwizer, Y. Okamoto, T. Heinisch, Y. Gu, M. M. Pellizzoni, V. Lebrun, R. Reuter, V. Köhler, J. C. Lewis and T. R. Ward, *Chem. Rev.*, 2018, **118**, 142–231.
3 E. Marcos, B. Basanta, T. M. Chidyausiku, Y. Tang, G. Oberdorfer, G. Liu, G. V. T. Swapna, R. Guan, D.-A. Silva, J. Dou, J. H. Pereira, R. Xiao, B. Sankaran, P. H. Zwart, G. T. Montelione and D. Baker, *Science*, 2017, **355**, 201–206.
4 D. Röthlisberger, O. Khersonsky, A. M. Wollacott, L. Jiang, J. DeChancie, J. Betker, J. L. Gallaher, E. A. Althoff, A. Zanghellini, O. Dym, S. Albeck, K. N. Houk, D. S. Tawfik and D. Baker, *Nature*, 2008, **453**, 190–195.
5 P. Srivastava, H. Yang, K. Ellis-Guardiola and J. C. Lewis, *Nat. Commun.*, 2015, **6**, 7789.
6 X. Garrabou, D. S. Macdonald, B. I. M. Wicky and D. Hilvert, *Angew. Chem., Int. Ed.*, 2018, **57**, 5288–5291.
7 J. Podtetenieff, A. Taglieber, E. Bill, E. J. Reijerse and M. T. Reetz, *Angew. Chem., Int. Ed.*, 2010, **49**, 5151–5155.
8 S. D. Khare, Y. Kipnis, P. J. Greisen, R. Takeuchi, Y. Ashani, M. Goldsmith, Y. Song, J. L. Gallaher, I. Silman, H. Leader, J. L. Sussman, B. L. Stoddard, D. S. Tawfik and D. Baker, *Nat. Chem. Biol.*, 2012, **8**, 294–300.
9 B. S. Der, D. R. Edwards and B. Kuhlman, *Biochemistry*, 2012, **51**, 3933–3940.
10 M. L. Zastrow, A. F. A. Peacock, J. A. Stuckey and V. L. Pecoraro, *Nat. Chem.*, 2012, **4**, 1–6.
11 M. L. Zastrow and V. L. Pecoraro, *J. Am. Chem. Soc.*, 2013, **135**, 5895–5903.
12 W. J. Song and F. A. Tezcan, *Science*, 2014, **346**, 1525–1528.
13 S. Studer, D. A. Hansen, Z. L. Pianowski, P. R. E. Mittl, A. Debon, S. L. Guffy, B. S. Der, B. Kuhlman and D. Hilvert, *Science*, 2018, **362**, 1285–1288.
14 J. Bos, F. Fusetti, A. J. M. Driessen and G. Roelfes, *Angew. Chem., Int. Ed.*, 2012, **51**, 7472–7475.
15 J. Bos, A. Garcìa-Herraiz and G. Roelfes, *Chem. Sci.*, 2013, **4**, 3578–3582.
16 I. Drienovská, L. Alonso-Cotchico, P. Vidossich, A. Lledós, J.-D. Maréchal and G. Roelfes, *Chem. Sci.*, 2017, **8**, 7228–7235.
17 D. N. Bolon and S. L. Mayo, *Proc. Natl. Acad. Sci. U. S. A.*, 2001, **98**, 14274–14279.
18 F. Richter, R. Blomberg, S. D. Khare, G. Kiss, A. P. Kuzin, A. J. T. Smith, J. Gallaher, Z. Pianowski, R. C. Helgeson, A. Grjasnow, R. Xiao, J. Seetharaman, M. Su, S. Vorobiev, S. Lew, F. Forouhar, G. J. Kornhaber, J. F. Hunt, G. T. Montelione, L. Tong, K. N. Houk, D. Hilvert and D. Baker, *J. Am. Chem. Soc.*, 2012, **134**, 16197–16206.
19 A. Rauwerdink and R. J. Kazlauskas, *ACS Catal.*, 2015, **5**, 6153–6176.
20 N. Preiswerk, T. Beck, J. D. Schulz, P. Milovnk, C. Mayer, J. B. Siegel, D. Baker and D. Hilvert, *Proc. Natl. Acad. Sci. U. S. A.*, 2014, **111**, 8013–8018.
21 S. Abe and T. Ueno, *RSC Adv.*, 2015, **5**, 21366–21375.
22 A. R. D. Voet, H. Noguchi, C. Addy, D. Simoncini, D. Terada, S. Unzai, S.-Y. Park, K. Y. J. Zhang and J. R. H. Tame, *Proc. Natl. Acad. Sci. U. S. A.*, 2014, **111**, 15102–15107.
23 A. R. D. Voet, H. Noguchi, C. Addy, K. Y. J. Zhang and J. R. H. Tame, *Angew. Chem., Int. Ed.*, 2015, **54**, 9857–9860.
24 K. S. Broo, L. Brive, P. Ahlberg and L. Baltzer, *J. Am. Chem. Soc.*, 1997, **119**, 11362–11372.
25 L. Schoonen, K. S. van Esterik, C. Zhang, R. V. Ulijn, R. J. M. Nolte and J. C. M. v. Hest, *Sci. Rep.*, 2017, **7**, 14772.
26 J. A. Verpoorte, S. Mehta and J. T. Edsall, *J. Biol. Chem.*, 1967, **242**, 4221–4229.